Cement and Concrete Research 119 (2019) 132–140

Contents lists available at ScienceDirect

Cement and Concrete Research

journal homepage: www.elsevier.com/locate/cemconres

Hardened properties of 3D printed concrete: The influence of process parameters on interlayer adhesion

R.J.M. Wolfs*, F.P. Bos, T.A.M. Salet

Department of the Built Environment, Eindhoven University of Technology, Eindhoven, the Netherlands

ARTICLE INFO

Keywords:
3D printing
Hardened concrete
Bond strength
Interlayer adhesion

ABSTRACT

The technology of 3D Concrete Printing (3DCP) has progressed rapidly over the last years. With the aim to realize both buildings and civil works, the need for reliable mechanical properties of printed concrete grows. As a consequence of the additive manufacturing technique, 3D printed structures may consist of several layers that should exhibit bond to guarantee a safe structural design. This paper presents the results of an experimental study on the relation between the 3DCP process parameters and the bond strength of 3D printed concrete. The effect of 3 process parameters (interlayer interval time, nozzle height, and surface dehydration) on two mechanical properties (compressive strength and tensile strength, determined through flexural and splitting tests), has been established, in three perpendicular directions. A very limited influence of layer orientation was found for the given process-material combination, given a sufficiently short interlayer interval time. However, the bond strength between the layers reduced for increasing interlayer interval times. This was also reflected by the failure mode of the samples. The reduction in strength became more pronounced for the samples that were left uncovered during the interval time, exposed to drying. No clear relation was found between the height of the nozzle, and the bond strength between layers. The results of this study, in comparison to various other works on 3DCP, emphasize the need for standardization of test methods and characterization of 3D printed concrete, as individual process parameters clearly must be considered in relation to the applied material and other process parameters.

1. Introduction

The technology of 3D Concrete Printing (3DCP), an extrusion based additive manufacturing technique in which linear filaments of cementitious mortars are deposited on top of each other to gradually form objects without the aid of a formwork (Fig. 1), has progressed rapidly over the last years. The viability of this manufacturing method for actual structures in the domain of infrastructure, residential and utilitarian buildings is now being explored. The ambitions, such as the structure span or height, are being stretched continuously. For an overview of recent examples of in-use or close-to-use projects and plans reference is made to [1–3]. For these projects, it is increasingly important that functional performance meets regular quality, safety, and economy standards.

With the expansion of projects, there is also a growing need for reliable mechanical properties as input for structural calculations. Because the process is distinctively different from conventional concrete manufacturing methods, existing design codes may be insufficiently compatible with the specific properties of printed elements. Research by various authors has already shown the structural performance of printed concrete is directionally dependent and influenced by process parameters such as interlayer interval time, print head speed, and print nozzle height (see further discussion below). The growing use in actual projects implies the bandwidth of these and other process parameters that are likely to have an effect on the structural properties of the printed product, is widening. For instance, the environmental conditions such as temperature and relative humidity may vary significantly, as both off-site and on-site printing approaches have been adopted, of which the latter is often performed under minimally controlled conditions. Furthermore, interlayer interval times increase with object size and multi-session processes (i.e. finish on one day, stop, and continue on the next). It should also be noted that the main loading direction on printed elements (i.e. in the plane of the interfaces or perpendicular thereon) varies in different projects.

The current study thus aims at further developing the understanding of the relation between process parameters and mechanical properties of 3D printed concrete, as it is a basis for safe structural design. In particular, the effect of 3 process parameters (interlayer interval time,

* Corresponding author.
E-mail address: r.j.m.wolfs@tue.nl (R.J.M. Wolfs).

https://doi.org/10.1016/j.cemconres.2019.02.017
Received 14 September 2018; Received in revised form 14 January 2019; Accepted 27 February 2019
Available online 08 March 2019
0008-8846/ © 2019 Elsevier Ltd. All rights reserved.

Fig. 1. 3D Concrete Printing: a type of additive manufacturing in which linear filaments on cementitious mortars are deposited on top of each other to gradually form objects without the aid of a formwork.

nozzle height, and surface dehydration), on the mechanical properties compressive strength and tensile strength, has been established in three perpendicular directions, for a specific combination of 3DCP facility and material. The tensile strength has been derived by both flexural tensile tests, and tensile splitting test, in compliance with the variation of loading conditions of 3D printed structures in practice.

2. Theory

The layered build-up of printed objects, the lack of compaction, and the typical material compositions used in 3DCP processes, set this manufacturing technology apart from others in terms of structural properties. Numerous interfaces are introduced that should adhere sufficiently. As the characteristics of adhesion are principally determined by mechanical interaction, chemical bonding, and intermolecular and surface forces [4], an anisotropic dependency on process parameters such as interlayer interval time, nozzle height, and surface humidity, should be expected.

The presence of interfaces between concrete layers of different ages is a well-known phenomenon in concrete construction (although their strength is still subject of research [5,6]). It regularly occurs in in-situ cast projects, combinations of precast and in-situ cast parts of a structure, and repairs of concrete structures. Distinctive of these interfaces is that they occur between a hardened and a fresh concrete layer.

Design codes for structural concrete (e.g. NEN-EN 1992-1-1 [7] and the ACI 318–08 [8]) provide calculation guidelines to determine shear strength of such joints based on the compressive strength (of the weakest concrete), the acting normal stress, the surface roughness, and the presence of reinforcement crossing the interface. This approach is an application of shear friction theory and ignores the chemical bond as well as the effects of restrained shrinkage (caused by different curing conditions) and differential stiffness which have been pointed out as factors to take into account [9]. Furthermore, it is limited to shear strength and does not include the tensile strength of bonds.

In a RILEM State-of-the-Art report on repairs, Silferbrand et al. [10] identify at least 13 factors that affect tensile and shear bond strength. These factors are related to the concrete properties, the surface quality, the placement and curing procedures, and a number of factors that are associated specifically with repairs in infrastructure. It is noted that the influence of surface roughness on shear is much more significant than on the tensile strength of a bond. Furthermore, the surface moisture is an important aspect of surface preparation and should be within certain boundaries as the effects of either a too wet or a too dry surface are detrimental.

To explain the behaviour of interfaces between concrete of different ages, Xie et al. [11] have taken a microstructural approach, by showing through Scanning Electron Microscopy (SEM) in the nanometer range that three layers of different reaction products occur at the interface. The first layer lies inside the old concrete and has no harmful influence to the interface strength. The second layer is located at the boundary, containing mostly calcium hydroxide (Ca(OH)2), and is weaker than the bulk material. The third layer, situated in the young concrete, is weakly affected.

When the interlayer interval times in 3D printed concrete are sufficiently long (i.e. at least exceeding the initial setting time), for instance when a print is stopped on day 1, and continued on the next, or with very large prints with fast-setting mixtures, these factors of bond strength may be relevant in 3DCP as well. Generally, however, another situation may typically occur too: interfaces between two layers of fresh material (i.e. both before their initial setting time). This situation has been studied much less intensively. To avoid the occurrence of distinct layers in cast Self-Compacting Concrete and associated loss of mechanical strength that can be as much as 40% [12], Roussel & Cussigh [13] observed that the structuration rate (thixotropic behaviour) should remain below a threshold value to allow subsequent layers to mix, while the surface roughness also determines the extent of adhesion between casts. This was confirmed in experimental research by Megid & Khayat [14] on several SCC mixtures with varying structuration rates. Assaad [15] found that a structuration rate of $0.2\,\mathrm{Pa/s} < A_{thix} < 0.75\,\mathrm{Pa/s}$ results in a stable mixture that is not overly sensitive to stoppages or delays between casts. Considering this applies already to relatively fluid SCCs, it should be expected that for low- or no-slump mixtures used in 3DCP, the occurrence of layering would be all the more pronounced.

In relation to 3D concrete printing and similar processes, the effects of the manufacturing process on the hardened material properties have been studied by various authors. Le et al. [16], using an OPC based printable concrete mixed with fly ash and silica fume, studied the compressive and flexural strength in 3 mutually perpendicular directions, defined by the print process, to find that both strengths were directionally dependent. Subsequently, other studies found similar directional dependencies of compressive and flexural strengths [17–22].

Furthermore, Le et al. [16] investigated the tensile strength of the interlayers with varying interface interval times (i.e. the time between the depositions of two subsequent layers) and found a decreasing strength with increasing interval times. This is generally recognized as one of the key competing requirements in concrete printing: the interval time should remain short enough to allow sufficient layer bonding, while the construction rate of the object should be slow enough to allow the material to gain strength and stiffness and avoid inprint failure [23]. Panda et al. [21] also studied the interface strength as a parameter of interlayer interval time, but additionally included print head speed and print nozzle height as variables. They found decreasing interface tensile strengths for increasing interval time, print head speed and nozzle height, for a geopolymer mortar composition.

Kim et al. [24] name water-cement ratio, concrete viscosity, interlayer interval time and superimposed dead load as major influences of interface strength, evaluated in terms of fracture energy obtained from crack mouth opening displacement (CMOD) tests. For an OPC printable mixture with initial and final setting times of 90 and 220 min, respectively, they found limited strength and fracture energy reductions for interval times of 15 and 30 min (compared to 0 min as reference), but a considerable decrease for an interval time of 60 min – which is still well beneath the initial set time.

Nerella et al. [25,26] complemented mechanical testing with extensive SEM observations in the micrometre range. For two printable mixtures and interval times of 1 min, 10 min, and 1 day, they found increasing strength reductions, which in the case of one mixture was rather dramatic (from almost 50% for 1 min to over 90% for one day). The SEM observations show increasingly clear interfaces between layers for larger interval times. Marchment et al. [27] found that interface tensile strength for 3 different interval times correlated with basically

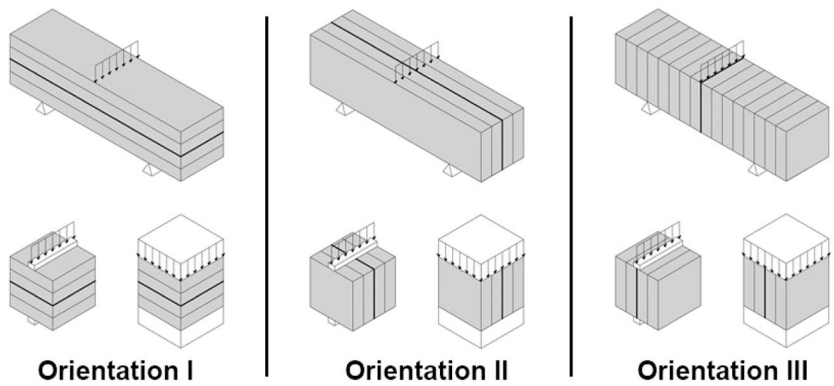

Fig. 2. 3D Printed layer orientations in flexural tension, tensile splitting, and compression tests. Note that for the compressive tests, orientation II and III have been combined into one sample series, as they are equal in terms of loading.

measured surface moisture content. Keita et al. report tensile splitting strength reductions of up to 50% for uncovered specimens, compared to specimens protected from drying [28].

In addition to the studies of the impact of 3DCP processing parameters on strength, the effect of these same parameters on durability is a topic of ongoing research. For instance, Schröfl et al. [29] address the increment of capillary water intake, for an increasing interlayer interval time up to 24 h. Van der Putten et al. [30] found an increasing porosity for larger interval times, as well as a decrease in bond strength, for interval times of 10 to 60 min. Bran-Anleu et al. [31] studied the chloride penetration in 3D printed specimens, which was found to be significantly higher for interval times of 24 h, compared to 2 min.

Clearly, a number of the identified factors that influence bond strength such as surface moisture, structuration level, perpendicular pressure and so forth can be influenced, willingly or unwillingly, through print process settings and conditions. For this study, interlayer interval time, nozzle height and surface dehydration were selected as test parameters as they were expected to constitute actual variations in individual print sessions (contrary to e.g. surface roughness that in different sessions with the same system and material is more likely to be the similar) that will significantly influence bond strength.

3. Method

An experimental program has been designed to study the impact of the layered interface in 3D printed structures using three destructive mechanical tests, namely flexural tension, tensile splitting, and cubic compression. The testing procedures have been based on existing mortar and concrete standards. However, as the specimen dimensions and corresponding loading conditions are typically not in line with the 3D concrete printing process, the procedures and dimensions were adjusted and scaled down where needed, for instance to prevent the presence of horizontal interfaces in samples to unduly influence the results.

3.1. Material, print process, and sample preparation

In this research, a custom designed printable mortar Weber 3D 145–2 was applied, containing Portland cement (CEM I 52.5 R), siliceous aggregate with a maximum particle size of 1 mm, limestone filler, additives, rheology modifiers and a small amount of polypropylene (PP) fibres. The water to fines (cement + fillers) ratio equals 0.495.

The samples were created using the 3DCP setup of the Eindhoven University of Technology (TU/e) [2]. This setup consists of a 4 degree of freedom (DOF) gantry robot and an M-Tec Duomix 2000 mixer-pump with a linear displacement pump, that feeds concrete through a Ø1 inch, 10 m length hose. All samples were taken from rectangular print objects consisting of layers 50 mm wide and 9.5 mm high. After printing, all objects were stored under a plastic sheet for 24 h. At an age of 1 day, they were removed from the print bed and saw-cut to obtain the specimens in their required dimensions, and to smoothen the loading and support surfaces to prevent occurring peak stresses due to the layered surface texture. After sawing, the samples were stored in water to maintain an equal curing history for all specimens, until testing at an age of 7 days.

3.2. Test program and parameter studies

The test program was designed in a manner to efficiently allow several comparative parameter studies of process parameters, mechanical properties, and directions:

- **Process parameters:**
  - o Interlayer interval time: 15 s, 1 h, 4 h, 7 h, 24 h
  - o Nozzle height: 8.0 mm, 9.5 mm, 11 mm
  - o Surface dehydration: covered, uncovered
- **Mechanical properties**: Compressive strength, flexural tensile strength, splitting tensile strength
- **Loading directions**: I, II, III

For each parameter, several values were selected for arguments provided below. Cast specimens were manufactured and tested as well, for reference purposes. They were cast into standard 40 × 40 × 160 mm mortar prisms, and considered to be directionally independent. As they did not feature interfaces, they were also independent of interlayer interval time and surface coverage. Each experimental series consisted of 7 specimens. In total 192 tests were performed.

The first parameter study concerned the effect of loading direction relative to layer orientation. Along with cast specimens, printed samples have been subjected to flexural tension, tensile splitting and compression tests, in three mutually perpendicular orientations related to the printing process, I, II, and III (Fig. 2). These samples were printed with an interlayer interval time of 15 s, i.e. all samples have been printed in one continuous process. The interval time of 15 s follows from the shortest possible printing time, given the specimen dimensions. The surface was not covered between the deposition of subsequent layers as dehydration was not considered relevant in such a short time period, and covering was not practically possible. The height of the nozzle in relation to the previous layer was put at the default value of 9.5 mm.

In the second study, the impact of the interlayer interval time was targeted. All samples had one *critical interface*, where the interlayer interval time was increased to respectively 1 h, 4 h, 7 h, and 24 h, for bending tests, and to 4 h and 24 h for splitting tensile tests. These interval times correspond globally with typical turning points in the

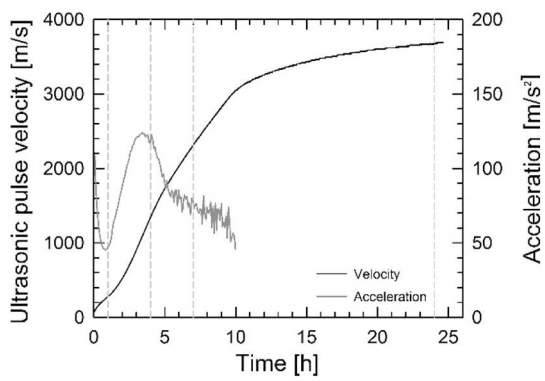

Fig. 3. Ultrasonic Pulse Velocity measurements on printed concrete, where the dashed lines indicate the printing sessions to reach specific interlayer interval times.

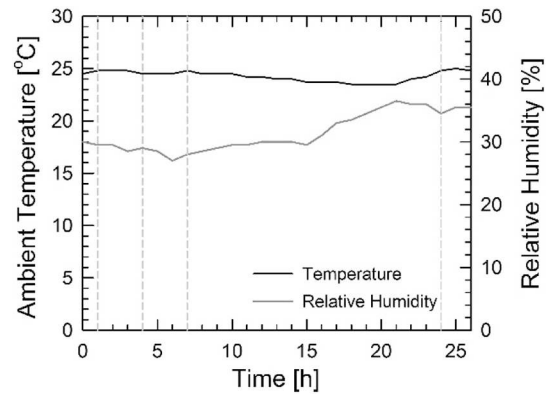

Fig. 4. Ambient temperature and relative humidity during printing, where the dashed lines indicate the printing sessions to reach specific interlayer interval times.

concrete hydration of the applied mortar. It was expected that this might result in significantly different results between the studied intervals. Ultrasonic wave transmission tests that have been performed on samples from the same print session (Fig. 3; method described in [32]) show that the 1 h interval print is just before the initial set time (when hydration reactions accelerate), the 4 h interval is at the reactions acceleration peak, the 7 h interval is when the reactions have decelerated, and the 24 h interval is after the reactions have slowed down significantly and the degree of hydration steadily increases. During the time gap in between printing, all samples were thoroughly covered by plastic sheet to prevent surface dehydration. All tests were performed in layer orientation III, which leaves the critical interface loaded in tension.

Subsequently, the effect of nozzle height on the flexural tensile strength in the III-direction (perpendicular to the interface surface) was studied. This parameter was expected to influence the bond between layers, based on observations during printing with various nozzle designs by the authors [33], and for different nozzle heights by Panda et al. [21]. The position of the nozzle was either deliberately lowered to 8.0 mm ('pushing' the new layer into the previous one), or increased to 11 mm ('dropping' the new layer onto the previous one), compared to the default nozzle height of 9.5mm. This study was performed for an interlayer interval times of 15 s and 24 h.

The fourth and final parameter study concerned the impact of surface dehydration, again tested on the flexural tensile strength in the III-direction. Here, samples with an interlayer interval time of 4 h and 24 h were left uncovered between the deposition of subsequent layers. The results were compared to those of printed samples that were completely covered during the interval time. The environmental temperature and relative humidity were approximately constant during these experiments, see Fig. 4, and on average equal to 24 °C and 32% respectively.

3.3. Flexural tension tests

Three-point bending tests were performed on prismatic specimens, according to NEN-EN 196-1 [34], to determine the flexural tensile strength. The printed specimens were saw-cut to dimensions of 40 × 40 × 160 mm, and loaded in an Automax loading rig with a rate of 50 N/s until failure. As prescribed, the free span l between supports is equal to 100 mm, and the loading is applied in the middle of the specimen. At failure, the load F_f is recorded and used to calculate the flexural tensile strength f_f of the specimen as follows:

$$f_f = \frac{3\,F_f \times l}{2\,b^3}$$

where:

I distance between supports, here equal to 100 mm, and

b side of the squared section, here equal to 40 mm

3.4. Tensile splitting tests

Tensile splitting tests were performed on cubic specimens, according to NEN-EN 12390-6 [35], albeit in a scaled down size of 40 × 40 × 40 mm, to accommodate for the dimensions as used in the 3DCP process. The packing strip and loading rate were scaled down accordingly. The samples were loaded with a rate of 125.7 N/s in a Schenk loading rig with a capacity of 100 kN. At failure, the load F_s was recorded and used to calculate the splitting tensile strength f_s of the specimen as follows:

$$f_s = \frac{2 \times F_s}{\pi \times L \times d}$$

where:

L length of the line of contact of the specimen, here equal to 40 mm, and

d designated cross-sectional dimensions, here equal to 40 mm.

Care was taken to position the specimens so that the critical interface was positioned exactly in the line of the load. However, linear FE analyses showed that even if the interface would be up to several millimetre of-centre, the peak tensile stress load acting on it would remain approximately equal and act on an almost identical area of the interface.

3.5. Compression tests

Likewise, 40 × 40 × 40 mm cubic specimens were used for compression tests based on the NEN-EN 12390-3 [36], but with scaled dimensions and a loading rate of 960 N/s. The same test rig was used. At failure, the load F_c was recorded and used to calculate the compressive strength f_c of the specimen as follows:

$$f_c = \frac{F_c}{A_c}$$

where:

A_c is the cross-sectional area of the specimen, here equal to 1600 mm^2

4. Results and discussion

The results of the experimental program will be discussed for each parameter study in the following subsections. Additionally, all results have been summarized in Table 1. The variations found in measured dimensions and densities were small and considered insignificant for both the printed and cast specimens, and were thus excluded from further discussions.

Table 1
Overview of test results, with average values μ, standard deviation SD, and relative standard deviation RSD.

Test	Orientation	Interval time	Nozzle height	Dehydration	Strength [MPa]		
					μ	*SD*	*RSD*
Flexural Tension		Cast specimen			4.28	0.31	7%
Flexural Tension	I	15 s	9.5 mm	Covered	4.29	0.25	6%
Flexural Tension	II	15 s	9.5 mm	Covered	4.70	0.45	10%
Flexural Tension	III	15 s	9.5 mm	Covered	3.68	0.14	4%
Flexural Tension	III	1 h	9.5 mm	Covered	3.51	0.40	11%
Flexural Tension	III	4 h	9.5 mm	Covered	3.48	0.50	14%
Flexural Tension	III	7 h	9.5 mm	Covered	3.34	0.48	15%
Flexural Tension	III	24 h	9.5 mm	Covered	3.10	0.43	14%
Flexural Tension	III	15 s	8 mm	Covered	3.92	0.30	8%
Flexural Tension	III	15 s	11 mm	Covered	3.98	0.24	6%
Flexural Tension	III	24 h	8 mm	Covered	2.65	0.78	29%
Flexural Tension	III	24 h	11 mm	Covered	2.35	0.63	27%
Flexural Tension	III	4 h	9.5 mm	Uncovered	1.72	0.26	15%
Flexural Tension	III	24 h	9.5 mm	Uncovered	2.28	0.23	10%
Tensile Splitting		Cast specimen			4.11	0.19	5%
Tensile Splitting	I	15 s	9.5 mm	Covered	3.68	0.16	4%
Tensile Splitting	II	15 s	9.5 mm	Covered	3.72	0.32	9%
Tensile Splitting	III	15 s	9.5 mm	Covered	3.55	0.26	7%
Tensile Splitting	III	4 h	9.5 mm	Covered	3.45	0.29	8%
Tensile Splitting	III	24 h	9.5 mm	Covered	2.80	0.37	13%
Compression		Cast specimen			42.30	2.36	6%
Compression	I	15 s	9.5 mm	Covered	28.51	1.70	6%
Compression	II, III	15 s	9.5 mm	Covered	29.19	1.84	6%

4.1. Layer orientation

The average results of the flexural tensile tests, tensile splitting tests, and compressive tests are given in Fig. 5, for three orientations, along with the reference cast specimens. Note that for the compressive tests, orientation II and III have been combined into one sample series consisting of 14 specimens as they are equal in terms of loading.

In the flexural tests, it was observed that orientation III is modestly weaker than the other two directions. An average strength reduction of 14% compared to direction I (print direction) was found. This reduction is limited in comparison to results presented by Le et al. [16] and Panda et al. [20] that reported flexural strength differences of up to around 50%.

Remarkably, the directional tensile strength dependency was not replicated by the splitting tensile test. Although a slight average reduction

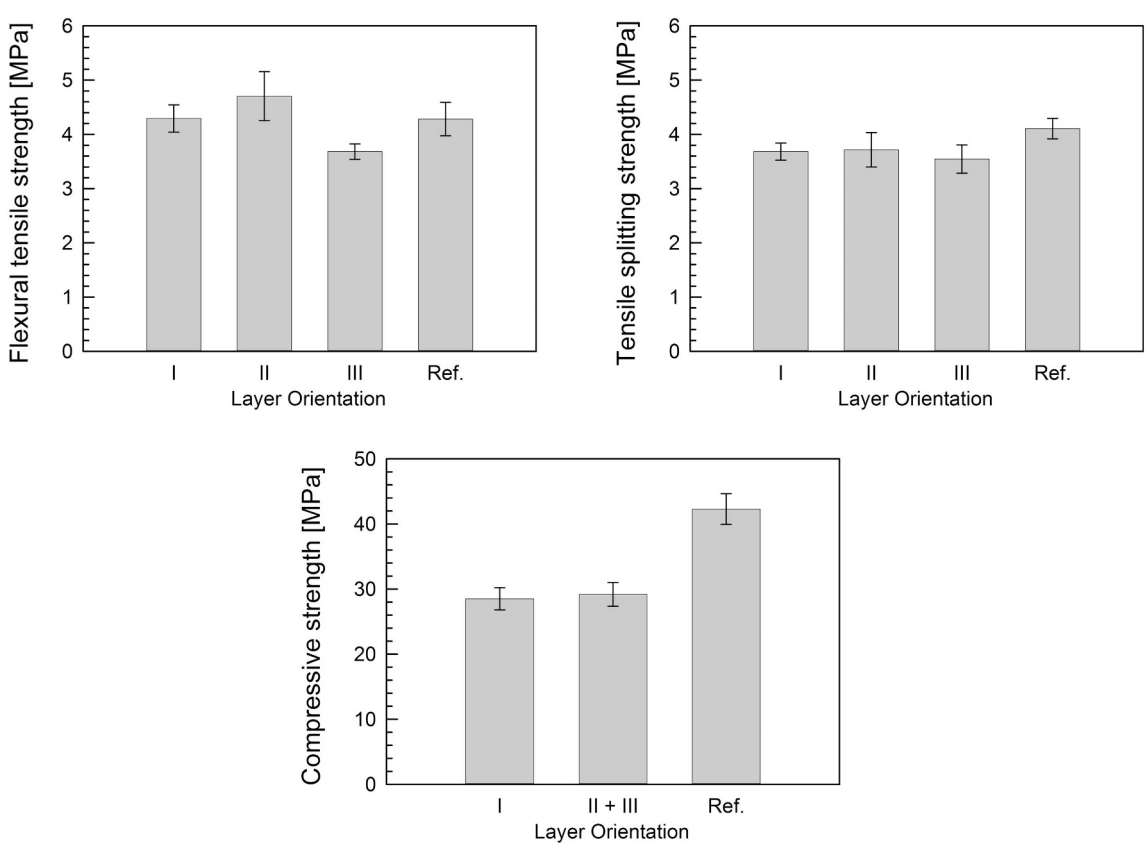

Fig. 5. Layer orientation results for flexural tension, tensile splitting, and compression tests. The interlayer interval time was equal to 15 s for all specimens.

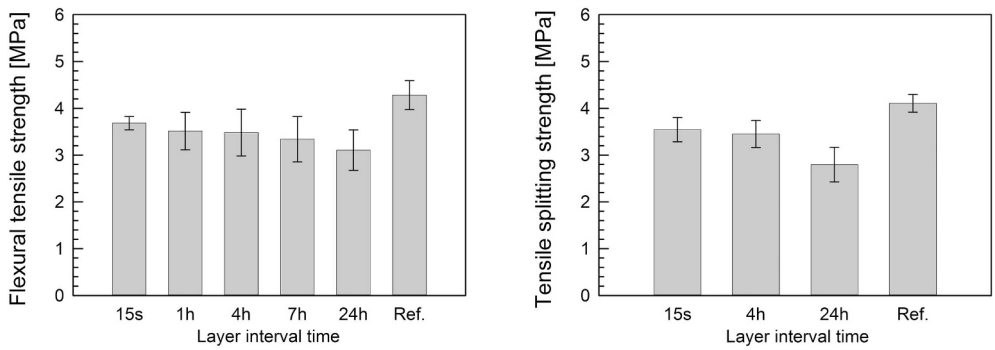

Fig. 6. Layer interval time results for flexural tension (left) and tensile splitting (right). With the exception of the 15 s interlayer interval time, all specimens have been covered for the duration of the time gap in between printing.

was found in that test, it was not significant given the scatter in individual results. Besides the general notion that the applied material-process combination in this study seems relatively robust with regard to directional strength dependencies, it is yet unclear what causes this difference in findings between both tensile tests. In any case, it seems that in the applied combination and for a relatively short time interval, a very limited tensile strength loss should be expected that for practical engineering purposes could be taken into account through a reduction factor.

For the compressive strength, no directional dependency was found. Of the cast specimens, only the compressive strength was considerably higher (approximately 31%) than that of the printed specimens. This is in line with other research [16,17].

4.2. Time interval

The average results of the flexural and splitting tests for various layer interval times are plotted in Fig. 6. Clearly, the strength reduces as the layer interval time increases. In the flexural tests, a reduction of 16% is measured at the 24 h interval, compared to the 15 s specimens. Likewise, a reduction of 21% is observed in the splitting test results.

For the layer interval times of 1 h and 4 h, only a minor drop in strength is observed in both tests, indicating that even if the print process is delayed for a significant period of time, the strength properties remain approximately equal, given adequate covering of the specimens during this period.

The impact of the interlayer interval time is not only observed in the failure strength, but also in the failure mode of the specimens. Typical failure modes are shown in Figs. 7 and 8 for flexural and splitting tests respectively. The relatively short interval times show a crack initiating at the lower bottom of the sample and propagating randomly through the samples, as is observed in the reference specimens. The higher interval times however, show a much more distinct vertical crack, positioned at the interface of two layers.

The reduction of strength for increasing interlayer interval times is

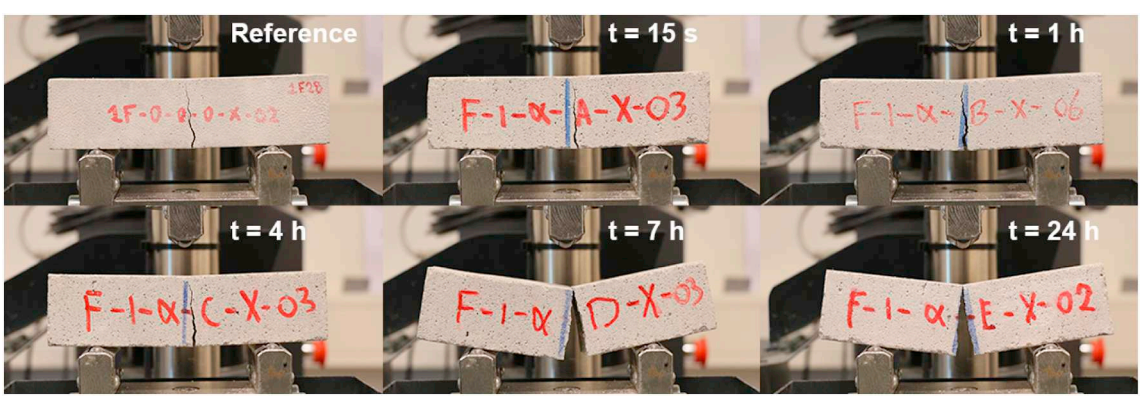

Fig. 7. Failure patterns in flexural tests for various interlayer interval times.

Fig. 8. Failure patterns in splitting tests for various interlayer interval times.

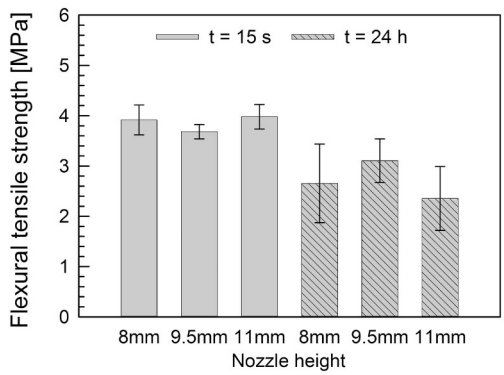

Fig. 9. Impact of 3 different nozzle heights for time interval of 15 s and 24 h.

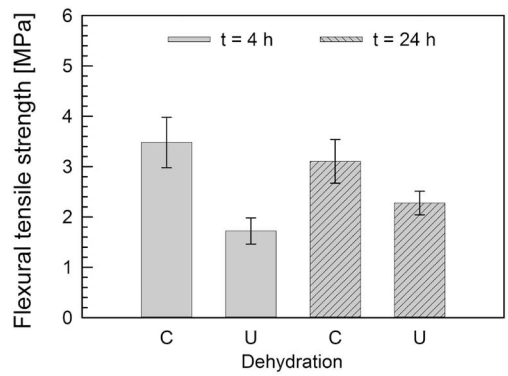

Fig. 10. Impact of sample dehydration for covered (C) and uncovered (U) samples for time interval of 4 h and 24 h.

in accordance with findings by other researchers. However, a quantitative comparison of these studies indicate that the interlayer interval time cannot be considered as an independent value, but should be considered in relation to the material and other process parameters adopted in each study. For instance, reductions up to 72% have been reported for the interlayer interval time of 60 min by Kim et al. [24], while the results of Panda et al. indicate 75% reduction at in interval time of 20 min [21]. In comparison, the reductions found in the current study are thus quite modest and the studied process-material combination seems rather robust in terms of interlayer interval time sensitivity.

4.3. Nozzle height

The effect of the nozzle height, studied by flexural tests, is presented in Fig. 9. For both the 15 s and 24 h interlayer time interval, no clear relation can be derived for the impact of the nozzle height on the specimen strength. In fact, the results only appear to become more scattered as the height is deviated from the default, preferred, setting. This may be attributed to the uncontrolled positioning of the layers, where the contact pressure and surface becomes variable. The layer quality reflects this variability, where layers are squeezed and deformed at lower nozzle heights, and inaccurately 'dropped' as the height increases.

The independency of strength on nozzle height is not in accordance with findings by Panda et al., who report a reduction of over 30% for increasing nozzle heights. However, the corresponding scatter in their results also significantly increased [21]. The observations of the authors in previous printing experiments indicated a stronger effect of the nozzle height compared to the results of this study. However, those experiments were performed with a different mixture, *Weber 3D 115-1,* with a significantly higher initial yield strength. In line with the findings on distinct layer casting by Roussel & Cussingh [13], the impact of nozzle height and design may indeed be more pronounced for material with higher initial yield value and structuration rate.

4.4. Dehydration

The flexural tensile strengths for covered and uncovered specimens are presented in Fig. 10, for an interlayer interval time of 4 h and 24 h. A clear impact of the specimen dehydration is recognized. This was also observed by optical microscope analysis of the crack surface, as illustrated in Fig. 11 for an interlayer interval time of 4 h. The uncovered samples showed a much smoother crack surface, along with a higher void content, compared to the covered specimens with the same interlayer interval times.

A drop of 51% and 26% in strength is measured for 4 h and 24 h respectively, compared to the covered specimens that were printed with the same interlayer interval time. Surprisingly, this reduction is stronger for the shorter interval time. A larger in reduction at 24 h was expected, as those samples were left uncovered for a longer time, thus allowing for more dehydration compared to the 4 h specimens. This indicates the presence of other environmental parameters that may influence the surface dehydration, for instance the air flux in the 3DCP facility, which was not controlled for this experimental program.

Nevertheless, this significant reduction in strength emphasizes the need for a controlled printing process and environment, as large reductions in structural properties may occur, even after 4 h interval where no significant strength loss was measured in case of proper covering (see Section 4.2). Actually, of all studied parameters, the dehydration with longer interlayer interval times has turned out to have the most prominent quantitative effect on flexural strength. Similar results were found by Keita et al., who report strength reductions of up to 50% after a couple tens of minutes for uncovered specimens found by tensile splitting tests [28]. Likewise, Nerella et al. reported reductions up to 90% for uncovered specimens with an interlayer interval time of 24 h [25].

Considering the fact that fast setting materials with high temperature increments due to rapid chemical reactions and in-site printing in uncontrolled environments are also applied in 3DCP practice, the more general conclusion from these results is that the impact of potential dehydration of the interface surfaces during printing should be explicitly addressed when planning the print process to ensure the structural safety of printed objects. Isotropic materials properties can only be ensured at short intervals or with thoroughly covered layer surfaces at longer intervals.

5. Summary and conclusions

An extensive experimental study has been performed to map the influence of various process parameters on the mechanical performance of 3D printed concrete. The bond strength between the layers is of particular interest, as this value appears to be critical for structural analysis of printed objects. The results of this study indicate a clear impact of the manufacturing process on the strength between layers.

From this study, only a very limited influence of layer orientation was found for the given process-material combination, if the interlayer interval time is sufficiently short. However, as the interlayer interval time increased, the bond strength between the layers reduces. This was also reflected by the failure mode of the samples. The reduction in strength became more pronounced for the samples that were left uncovered during the interval time, susceptible to drying, before the subsequent layers were printed. Finally, no clear relation was found between the height of the nozzle, and the bond strength between layers.

Some findings were in line with expectations based on available literature on both (non-printed) bonded concrete, and relatively limited work on interface strength in 3D printed concrete. However, certain process parameter results only corresponded quantitatively, while other

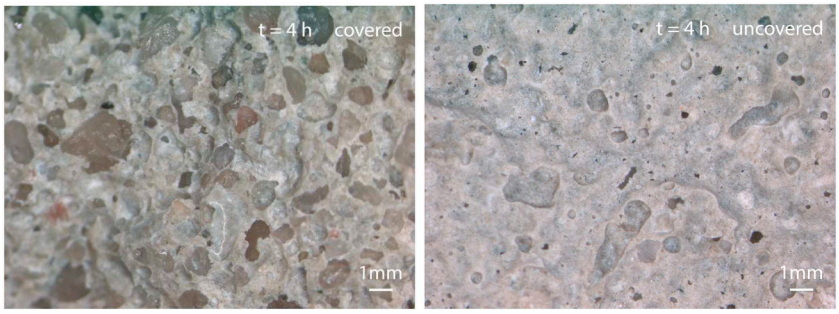

Fig. 11. Optical microscope observations on the crack surface of covered (left) and uncovered (right) specimens, for interlayer interval time of 4 h.

parameters proved to be insignificant for the 3DCP setup and material as used for this study. In general, the applied material-process combination appears to be relatively robust in terms of the effects of several parameters on the flexural tensile, splitting tensile and compressive strength, with the exception of dehydration of the interface surface which, for longer interval times, can cause significant strength reductions. It should be noted however, that in practice the influence of the studied process parameters may be stronger, as the results presented here were based on ideal curing conditions, which deviates from the typical (uncontrolled) environments of 3D concrete printers in practice.

When comparing results of various studies, it becomes clear that individual process parameters, for instance interlayer interval time, cannot be considered independently of the applied material and other process parameters. This emphasizes the need for standardization of test methods and characterization of 3D printed concrete, as called for by Buswell et al. [3].

Considering the realized and upcoming projects manufactured by 3DCP and affiliated digital manufacturing techniques using concrete, this study underlines the need for quality control methods. The structural integrity of the end result greatly depends on a number of process parameters, which can be difficult to predict or control in practice. Real-time measurement and feedback systems will have to be incorporated into the manufacturing process, to fulfil the required safety standards and be economically competitive.

Acknowledgements

The support of the staff of the Structures Laboratory Eindhoven is greatly acknowledged. The assistance in the 3DCP research of Master track students Structural Design at the TU/e Department of the Built Environment is highly valued. For this paper, the authors appreciate the work of J.H.F. van Alebeek and K. Nefs in particular, for their assistance in the experimental work.

The TU/e research program on 3D Concrete Printing is co-funded by a partner group of enterprises and associations, that on the date of writing consisted of (alphabetical order) Ballast Nedam, BAM Infraconsult bv, Bekaert, Concrete Valley, CRH, Cybe, Saint-Gobain Weber Beamix, SGS Intron, SKKB, Van Wijnen, Verhoeven Timmerfabriek, and Witteveen + Bos. Their support is gratefully acknowledged.

References

[1] N. Labonette, A. Rønnquist, B. Manum, P. Rüther, Additive construction: state-of-the-art, challenges and opportunities, Autom. Constr. 72 (3) (2016) 347–366.
[2] F.P. Bos, R.J.M. Wolfs, Z.Y. Ahmed, T.A.M. Salet, Additive manufacturing of concrete in construction: potentials and challenges, Virtual Phys Prototyp. 11 (3) (2016) 209–225.
[3] R.A. Buswell, W.R. Leal de Silva, S.Z. Jones, J. Dirrenberg, 3D printing using concrete extrusion: a roadmap for research, Cem. Concr. Res. 112 (2018) 37–49.
[4] M. Fiebrich, Grundlagen der Adhäsionskunde, Deutscher Ausschuss für Stahlbeton 334 (1994) 75–90.
[5] R. Norbert, S. Csaba, Experimental Investigations on Upgrading Structures with High Strength, in IABSE Symposium, Rotterdam 2013: Assessment, Upgrading and Refurbishment of Infrastructures, Rotterdam (2013).
[6] R. Ralf, Z. Konrad, Capacity of Shear Joints in Applications of High Performance Concrete in Strengthening and Retrofitting of old Concrete Structures, IABSE Symposium, Melbourne 2002: Towards a Better Built Environment — Innovation, Sustainability, Information Technology, Melbourne, 2002.
[7] NEN-EN 1991-1, Eurocode 2: Design of Concrete Structures — Part 1–1: General Rules and Rules for Buildings.
[8] ASTM 318-08, Building Code Requirements for Structural Concrete and Commentary.
[9] P.M.D. dos Santos, Assessment of the Shear Strength between Concrete Layers, PhD thesis University of Coimbra, Portugal, 2009.
[10] J. Silfwerbrand, H. Beushausen, L. Courard, Chapter 4, Bond, in: B. Bissonnette, et al. (Ed.), Bonded Cement-Based Material Overlays for the Repair, the Lining or the Strengthening of Slabs or Pavements, RILEM State-of-the-Art Reports 3, 2011, pp. 51–79.
[11] H. Xie, G. Li, G. Xiong, Microstructure model of the interfacial zone between fresh and old concrete, Journal of Wuhan University of Technology - Mater. Sci. Ed. 17 (4) (2002) 64–68.
[12] P. Coussot, N. Roussel, Quantification de la thixotropie des matériaux cimentaires et de ses effet, Revue Européenne de Génie Civil 10 (1) (2006) 45–63.
[13] N. Roussel, F. Cussingh, Distinct-layer casting of SCC: the mechanical consequences of thixotropy, Cem. Concr. Res. 38 (2008) 624–632.
[14] W.A. Megid, H.K. Kamal, Bond strength in multilayer casting of self-consolidating concrete, ACI Mater. J. 114 (3) (2017) 467–476.
[15] J.J. Assaad, Correlating thixotropy of self-consolidating concrete to stability, formwork pressure, and multilayer casting, J. Mater. Civ. Eng. 28 (10) (2016).
[16] T.T. Le, S.A. Austin, S. Lim, R.A. Buswell, R. Law, A.G.F. Gibb, T. Thorpe, Hardened properties of high-performance printing concrete, Cem. Concr. Res. 42 (2012) 558–566.
[17] P. Feng, X. Meng, J.F. Chen, L. Ye, Mechanical properties of structures 3D printed with cementitious powders, Constr. Build. Mater. 93 (2015) 486–497.
[18] V.M. Nerella, M. Krause, M. Näther, V. Mechtcherine, Studying printability of fresh concrete for formwork free Concrete onsite 3D Printing technology (CONPrint3D), Proceeding for the 25th Conference on Rheology of Building Materials, Regensburg, Germany, 2016.
[19] B. Zareiyan, B. Khoshnevix, Interlayer adhesion and strength of structures in contour crafting — effects of aggregate size, extrusion rate, and layer thickness, Autom. Constr. 81 (2017) 112–121.
[20] B. Panda, S.V. Paul, M.J. Tan, Anisotropic mechanical performance of 3D printed fiber reinforced sustainable construction material, Mater. Lett. (2017) (2019) 146–149.
[21] B. Panda, S.C. Paul, N.A.N. Mohamed, Y.W.D. Tay, M.J. Tan, Measurement of tensile bond strength of 3D printed geopolymer mortar, Measurement 113 (2018) 108–116.
[22] S.C. Paul, Y.W.D. Tay, B. Panda, M.J. Tan, Fresh and hardened properties of 3D printable cementitious materials for building and construction, Arch. Civ. Mech. Eng. 18 (2018) 311–319.
[23] R.J.M. Wolfs, F.P. Bos, T.A.M. Salet, Early age mechanical behaviour of 3D printed concrete: numerical modelling and experimental testing, Cem. Concr. Res. 106 (2018) 103–116.
[24] K. Kim, S. Park, W. Kim, Y. Jeong, J. Lee, Evaluation of shear strength of RC beams with multiple interfaces formed before initial setting using 3D printing technology, Materials 10 (2017) 1–22.
[25] V.N. Nerella, S. Hempel, V. Mechtcherine, Micro- and macroscopic investigations on the interface between layers of 3D-printed cementitious elements, International Conference on Advances in Construction Materials and Systems, Chennai, 2017.
[26] V. Nerella, S. Hempel, V. Mechtcherine, Effects of Layer-Interface Properties on Mechanical Performance of Concrete Elements Produced by Extrusion-Based 3D-Printing, Prepint (2018).
[27] T. Marchment, M. Xia, E. Dodd, J. Sanjayan, B. Nematollahi, Effect of delay time on the mechanical properties of extrusion-based 3D printed concrete, 34th International Symposium on Automation and Robotics in Construction, 2017.
[28] E. Keita, H. Bessaies-Bey, W. Zuo, P. Belin, N. Roussel, Weak Bond Strength between Successive Layers in Extrusion-Based Additive Manufacturing: Measurement and Physical Origin, Extended Abstracts of 1st International Conference on Concrete and Digital Fabrication, Digital Concrete 2018, Zurich, 2018.
[29] C. Schröfl, V. Nerella, V. Mechtcherine, Capillary water intake by 3D-printed concrete visualised and quantified by neutron radiography, in: T. Wangler, R. Flatt

(Eds.), First RILEM International Conference on Concrete and Digital Fabrication – Digital Concrete 2018, Springer, Cham, 2019, pp. 217–224.
[30] v.d. Putten, J.G. de Schutter, K. Vvan Tittelboom, The effect of print parameters on the (micro)structure of 3D printed cementitious materials, in: T. Wangler, R. Flatt (Eds.), First RILEM International Conference on Concrete and Digital Fabrication – Digital Concrete 2018, Springer, Cham, 2019, pp. 234–244.
[31] P. Bran-Anleu, T. Wangler, R.J. Flatt, Chloride ingress through cold joints in digitally fabricated concrete by U-XRF mapping, Extended Abstracts of 1st International Conference on Concrete and Digital Fabrication, Digital Concrete 2018, Zurich, 2018.
[32] R.J.M. Wolfs, F.P. Bos, T.A.M. Salet, Correlation between destructive compression tests and non-destructive ultrasonic measurements on early age 3D printed concrete, Constr. Build. Mater. 181 (2018) 447–454.
[33] T.A.M. Salet, Z.Y. Ahmed, F.P. Bos, H.L.M. Laagland, Design of a 3D printed concrete bridge by testing, Virtual Phys. Prototyp. 13 (3) (2018) 222–236.
[34] NEN-EN 196-1, Methods of Testing Cement — Part 1: Determination of Strength.
[35] NEN-EN 12390-6, Testing Hardened Concrete — Part 6: Tensile Splitting Strength of Test Specimens.
[36] NEN-EN 12390-3, Testing Hardened Concrete — Part 3: Compressive Strength of Test Specimens.